

How the Fourteen Most Stable CH<sub>4</sub>P<sub>2</sub> Isomers Interconvert—An *ab Initio*/NMR Study

Alk Dransfeld,<sup>†</sup> Luc Landuyt,<sup>†</sup> Michaela Flock,<sup>‡</sup> Minh Tho Nguyen,<sup>\*,†</sup> and  
Luc G. Vanquickenborne<sup>†</sup>

University of Leuven, Department of Chemistry, Celestijnenlaan 200F, B-3001 Leuven, Belgium, and Technical University Graz, Institute of Inorganic Chemistry, Stremayrgasse 16/IV, A-8010 Graz, Austria

Received: February 3, 2000; In Final Form: September 14, 2000

Energies of minima and TS as well as characteristic NMR chemical shifts are reported for the parent *unsaturated* phospho-organic molecules with CP<sub>2</sub> backbone. Within the 14 relevant isomers of CH<sub>4</sub>P<sub>2</sub>, the two most stable structures are 1,2-diphospha-1-propene, **3**, and diphosphirane (cyclo-CH<sub>2</sub>(PH)<sub>2</sub>, **1**, *E*<sub>rel</sub> = 8 kJ/mol). The relative energies in kJ/mol at MP2/6-31G(d,p) are 84 for 1,3-diphospha-2-propene, 54 for 1,2-diphospha-2-propene, and for the phosphinidenes, they are 63 (P–PH–CH<sub>3</sub>) and 102 (P–CH<sub>2</sub>–PH<sub>2</sub>). Although the potential intermediate products (PH–CH<sub>2</sub>–PH, PH–PH–CH<sub>2</sub>, and cyclo-CH<sub>2</sub>–PH<sub>2</sub>–P) of diphosphirane rearrangements have the relative energies 182, 157, and 158 kJ/mol, respectively, and other minima were found to have *E*<sub>rel</sub> between 287 and 322 kJ/mol. Rupture of endocyclic bonds of **1a** displays a preference for opening the P–C bond toward the CH<sub>2</sub>–PH–PH structure, which is stabilized by allyl conjugation. The lowest energy pathway for isomerization of **1** has a barrier of 213 kJ/mol and goes via the intermediate cyclo-(CH<sub>2</sub>)(PH<sub>2</sub>)-(P) toward PH<sub>2</sub>–P=CH<sub>2</sub>. The calculated energy barriers of CH<sub>3</sub>–P=PH, **3**, indicate that this isomer should be kinetically stable as isolated molecule.

## Introduction

In P<sub>*n*</sub>C<sub>*m*</sub>H<sub>*r*</sub> molecules, the principles of organic and inorganic chemistry are combined. Although many phospho-organic compounds can be found in reviews,<sup>1,2,3,4,5</sup> the scope of potential structures in the fundamental systems C<sub>2</sub>H<sub>4</sub>P and CH<sub>4</sub>P<sub>2</sub> are not completely investigated (neither structural preferences nor kinetic stability). Synthetic attempts are probably hampered by overestimated relative energies based on ‘bond energies’.

The first CH<sub>4</sub>P<sub>2</sub> derivative was synthesized by Baudler<sup>6</sup> in 1977 by ionic [2+1] cyclocondensation of R<sub>2</sub>CCl<sub>2</sub> with a P<sub>2</sub>R'<sub>2</sub>K<sub>2</sub> salt. Similarly, addition of carbenes to diphosphene, RP=PR, leads to diphosphiranes (abbreviated as DPP in the following). An alternative synthetic pathway to DPP starts from 1,2-diphospha-2-propene<sup>7</sup> and is assumed to have methylenediphosphene intermediates. Recent experiments in which the diphosphirane ring is opened also revive the question as to whether the ring is the best structure for CH<sub>4</sub>P<sub>2</sub> and its derivatives. The formation of DPP via a proposed 1,2-diphosphaallyl intermediate<sup>7</sup> especially raises the question as to whether the ring is formed under thermodynamic or kinetic control. Only a few of the possible CR<sub>4</sub>P<sub>2</sub> isomers have been detected so far.<sup>5</sup> Therefore, a comprehensive investigation of the CH<sub>4</sub>P<sub>2</sub> energy hypersurface can provide suggestions for new products and reactive intermediates. Because the <sup>31</sup>P NMR chemical shifts of stable isomers can be *ab initio* calculated,<sup>8</sup> these data may assist in identification of unexpected species.

Previous theoretical investigations by Pfister-Guillouzo et al. (abbreviated as PG in the following)<sup>9,10,11</sup> considered some isomers of the parent CH<sub>4</sub>P<sub>2</sub><sup>10</sup> including biradical singlets,<sup>11</sup> the CH<sub>3</sub>P<sub>2</sub><sup>•</sup> radical, and the ions<sup>10</sup> CH<sub>3</sub>P<sub>2</sub><sup>−</sup> and CH<sub>3</sub>P<sub>2</sub><sup>+</sup>. Although

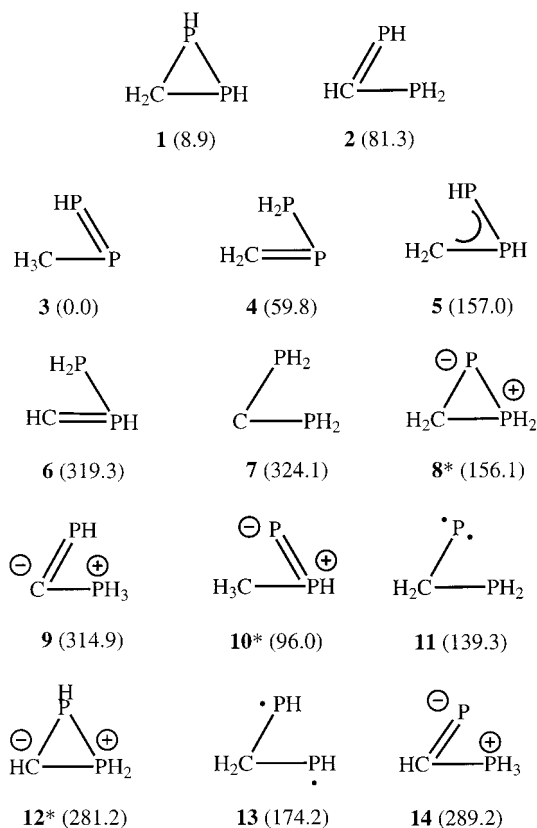


**Figure 1.** Structures and relative energies in kJ/mol of CH<sub>4</sub>P<sub>2</sub> isomers (The asterisk, \*, indicates that the formal charges do not reflect the actual charge distribution for **8**, **10**, and **12**).

the CH<sub>4</sub>P<sub>2</sub> isomers diphosphirane (**1** in Figure 1), the methyldiphosphinophosphinidene triplet, **10b**, 1,3-diphospha-propene, **2**, and methylenediphosphene, **5**, are reported to have the relative

\* To whom correspondence should be addressed. E-Mail: minh.nguyen@chem.kuleuven.ac.be

<sup>†</sup> University of Leuven, Department of Chemistry.

<sup>‡</sup> Technical University Graz, Institute of Inorganic Chemistry.

**TABLE 1: Total DFT and MP2 Energies<sup>a</sup>, Zero Point Vibrational Energy, ZPVE, and Relative Energies<sup>b</sup> of (CH<sub>4</sub>P<sub>2</sub>) Minimum Geometries 1 to 14**

structure	character <sup>c</sup>	DFT <sup>a</sup> $E_{\text{tot}}$	MP2 <sup>a</sup> $E_{\text{tot}}$	MP2 ZPVE	MP2 $E_{\text{rel}}^b$	MP2 $E_{\text{rel}+\text{z}}^b$
1a	1, C <sub>2</sub>	-723.201 00	-721.983 18	126.0	8.9	6.8
1b	1, C <sub>s</sub>	-723.197 76	-721.979 69	125.4	18.0	15.3
2a	1, C <sub>1</sub>	-723.172 88	-721.954 35	116.1	84.6	72.6
2b	1, C <sub>s</sub>	-723.170 11	-721.952 52	115.5	89.4	76.8
2c	1, C <sub>1</sub>	-723.174 20	-721.955 58	116.4	81.3	69.6
2d	1, C <sub>s</sub>	-723.171 45	-721.953 68	115.6	86.3	73.8
2e	3, C <sub>1</sub>	-723.113 59	-721.885 06	109.7	266.5	248.1
3a	1, C <sub>1</sub>	-723.205 47	-721.986 56	128.2	0.0	0.0
3b	1, C <sub>s</sub>	-723.200 50	-721.980 52	127.0	15.9	14.5
3c	3, C <sub>1</sub>	-723.160 12	-721.934 29	124.7	137.2	133.8
4a	1, C <sub>s</sub>	-723.185 20	-721.963 77	120.0	59.8	51.7
4b	3, C <sub>1</sub>	-723.126 73	-721.895 57	113.9	238.9	224.7
5a	1, C <sub>s</sub>	-723.151 10	-721.926 77	118.0	157.0	146.9
5b	1, C <sub>s</sub>	-723.149 08	-721.923 93	116.7	164.4	153.0
5c	3, C <sub>1</sub>	-723.128 96	-721.89822	113.5	231.9	217.3
6a	1, C <sub>1</sub>	-723.09002	-721.860 71	109.4	330.4	311.7
6b	1, C <sub>1</sub>	-723.096 10	-721.864 94	110.4	319.3	301.6
6c	1, C <sub>s</sub>	-723.090 02	-721.860 63	109.1	330.6	311.6
6d	1, C <sub>s</sub>	-723.094 81	-721.863 40	110.3	323.3	305.5
6e	3, C <sub>1</sub>	-723.081 08	-721.850 68	107.6	356.7	336.2
6f	3, C <sub>1</sub>	-723.076 88	-721.847 69	107.1	364.6	343.6
7a	1, C <sub>s</sub>	-723.096 29	-721.862 59	— <sup>d</sup>	325.5	— <sup>d</sup>
7b	1, C <sub>2</sub>	-723.096 56	-721.863 11	— <sup>d</sup>	324.1	— <sup>d</sup>
7c	3, C <sub>1</sub>	-723.081 89	-721.849 54	105.4	359.7	337.0
8	1, C <sub>s</sub>	-723.145 53	-721.927 11	126.2	156.1	154.2
9a	1, C <sub>s</sub>	-723.088 76	-721.866 77	111.9	314.5	298.3
9b	1, C <sub>s</sub>	-723.085 53	-721.862 92	110.6	324.6	307.1
9c	3, C <sub>1</sub>	-723.047 57	-721.811 49	107.5	459.6	439.0
10a	1, C <sub>s</sub>	-723.171 32	-721.950 01	129.0	96.0	96.9
10b	3, C <sub>1</sub>	-723.167 23	-721.947 11	129.0	103.6	104.5
11a	3, C <sub>s</sub>	-723.149 57	-721.933 49	122.8	139.3	134.3
11b	3, C <sub>1</sub>	-723.146 96	-721.931 89	122.9	143.5	138.3
12	1, C <sub>1</sub>	-723.099 65	-721.879 44	113.9	281.2	267.0
13a	3, C <sub>2</sub>	-723.140 27	-721.919 85	117.8	175.1	164.8
13b	3, C <sub>s</sub>	-723.140 50	-721.920 19	118.1	174.2	164.2
13c	3, C <sub>1</sub>	-723.138 08	-721.918 30	117.0	179.2	168.0
13d	3, C <sub>2v</sub>	-723.136 10	-721.916 60	116.1	183.7	171.6
14a	1, C <sub>s</sub>	-723.100 35	-721.876 41	118.1	289.2	279.2
14b	3, C <sub>1</sub>	-723.088 64	-721.867 13	117.1	313.6	302.6

<sup>a</sup> Total energies in Hartree at DFT, UB3LYP/6-31G(d,p)/UB3LYP/6-31G(d,p), and MP2, UMP2/6-31G(d,p)/UMP2/6-31G(d,p). The MP2 geometry parameters are provided in Figure 2. <sup>b</sup> Zero point vibrational energy, ZPVE, and relative energies in kJ/mol.  $E_{\text{rel}+\text{z}}$  is the relative energy on the energy hypersurface plus the vibrational energy. Relative energies in Figure 3 are without ZPVE correction. <sup>c</sup> Characteristics of the electronic structure (1 for singlet, 3 for triplet) and geometry (point group). <sup>d</sup> At UMP2, the energy hypersurface of **7** shallow. The symmetric structures are minima at CI level (see text). At MP2 the **7** symmetric singlets are partial optimized structures with relative energies of 6.5 for **7a** and 5.2 for **7b** with respect to the corresponding MP2 structures optimized without symmetry constrain.

energies 0, 35, 64, and 174 kJ/mol,<sup>10</sup> respectively, the lowest energy isomer, methyldiphosphane (**3**; 1,2-diphospha-1-propene), was only considered in a study by Schoeller<sup>12</sup> on the effect of a substituent “R” on the hydrogen bridging in P<sub>2</sub>H<sup>+</sup>R<sup>−</sup> systems. Isomers like 1,2-diphospha-2-propene, **4**, phosphamethylphosphinidene, **11**, and 2H-diphosphirane, **12**, were ignored in all previous investigations, despite being potentially important intermediates. In the most recent theoretical work, PG<sup>11</sup> investigated the alternative reaction paths from **1** to **2** with ab initio SCF–CI based on RHF/4-31+G(d) geometries. Here, we report a comprehensive set of CH<sub>4</sub>P<sub>2</sub> isomers together with refined transition structures and isomerization barriers at MP2-(fc)/6-31G(d,p)/MP2(fc)/6-31G(d,p) level. Furthermore, higher level geometry optimizations and ab initio calculated NMR chemical shifts are provided for selected molecules.

### Details of Computation

For the purpose of comparison, we have used ab initio molecular orbital methods at the same level as in the previous report on phosphirane<sup>13a</sup> and triphosphirane.<sup>13b</sup> MP2/6-31G(d,p) geometric parameters of the completely optimized structures

are presented in Figure 2; the corresponding total and relative energies are listed together with the zero point vibration energies in Table 1. The additional B3LYP/6-31G(d,p) energies (geometries are supplementary) are listed to see systematic differences with respect to the MP2 results for CH<sub>4</sub>P<sub>2</sub> and to be compared with the data for larger molecules (derivatives of the CH<sub>4</sub>P<sub>2</sub> isomers),<sup>14</sup> which cannot be computed at MP2 level with the available equipment. For the transition structures, TS, depicted in Figure 6 (including the trajectories of the vibration mode with negative force constant), the intrinsic reaction coordinates (IRC) were calculated to determine the two minima that are connected by the TS. In general, X/Y denotes a TS connecting both equilibrium structures X and Y (Table 2). For differentiation between the methyl and the hydrogen 1,2-shift between **3a** and **10a** the capital letters C (H, respectively) is added. The <sup>31</sup>P NMR chemical shifts computed with the GIAO method at B3LYP/6-311G(d) level on the MP2(fc)/6-31G(d,p) geometries are presented in Table 5. Throughout this paper, bond lengths are given in Angströms, bond angles in degrees, total energies in Hartrees, zero-point vibrational relative energies in kJ/mol, and chemical shifts in ppm. Unless otherwise stated, the energies cited in the text refer to the MP2/6-31G(d,p)/MP2/6-31G(d,p)

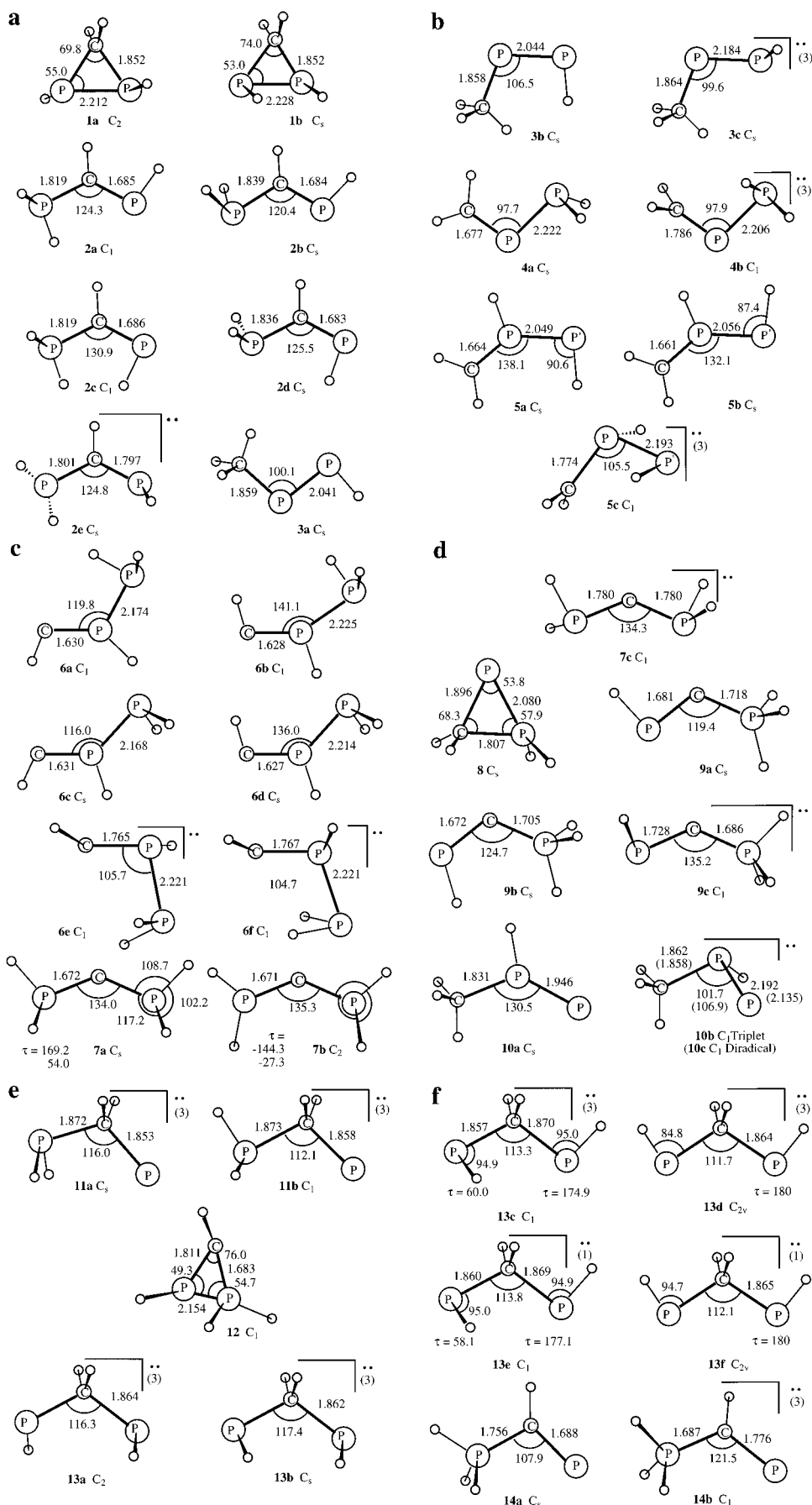


**Figure 2.** Geometries (bond length in Å; angles in degree) of  $CH_4P_2$  isomer minima.

calculations. Because one natural orbital (single determinant approach) cannot describe the electronic structure of diradicals

precisely, the MP2 calculations for **6e**, **6f**, **7c**, **9c**, **10c**, **13e**, and **13f** are only approximations ("pseudo-singlets") and the betain

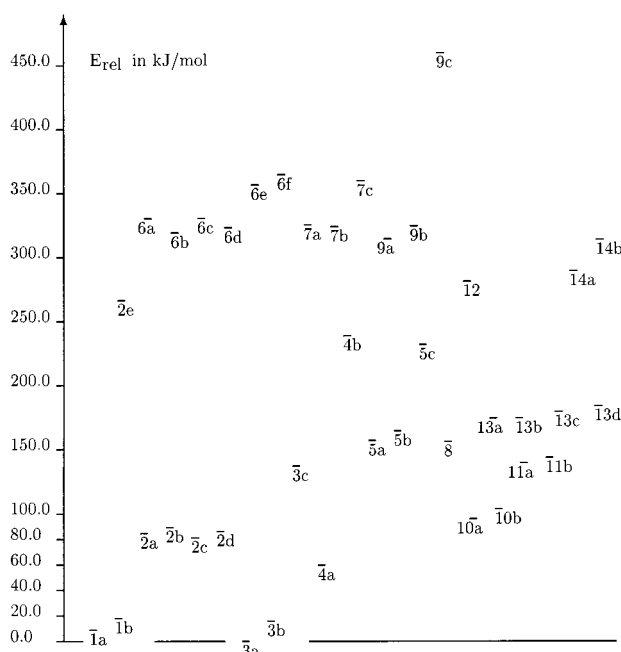


**Figure 3.** Energy diagram of CH<sub>4</sub>P<sub>2</sub> minimum structures ( $E_{\text{rel}}$  in kJ/mol).

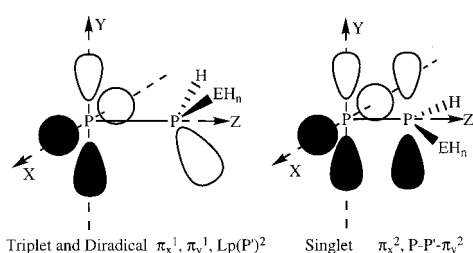


**Figure 4.** Orbital plot of the AOs involved in the frontier orbitals of P-PH-EH<sub>n</sub> type phosphinidenes with pyramidal or planar  $\sigma^3$ -P.

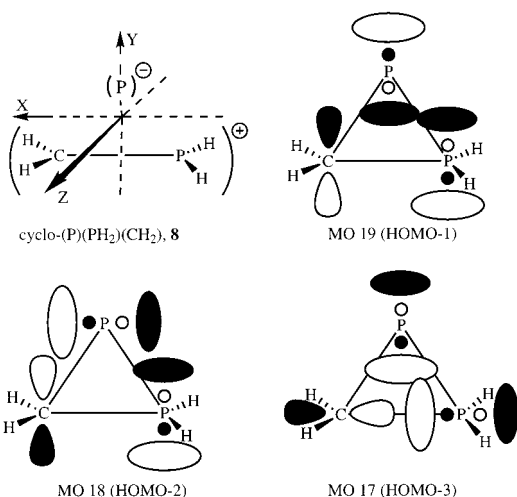


**Figure 5.** Orbital plot of the AOs involved in the frontier orbitals of cyclo-(P)(PH<sub>2</sub>)(CH<sub>2</sub>).

character of geometries **6a–d**, **7a**, **7b**, **9a**, **9b**, **10a**, and **14a** is overestimated. To check for the multiconfigurational character of selected geometries, single point RASSCF calculations were performed on CISD optimized structures. All RASSCF calculations were performed with the software package MOLCAS-4.0.<sup>15</sup> The ANO basis sets (denoted as ANO-S in the MOLCAS basis set library) were used. The active space consisted of 6 electrons in 6 orbitals (unless otherwise stated HOMO-1, HOMO, LUMO, and LUMO+1). All calculations, optimization,

**TABLE 2: Relative Energies<sup>a</sup> of Transition Structures<sup>b</sup>, TS, on the (CH<sub>4</sub>P<sub>2</sub>) Energy Hypersurface<sup>c</sup> at MP2/6-31G(d,p)**

TS <sup>b</sup>	character <sup>d</sup>	$E_{\text{rel},3}^e$	$E_{\text{rel},A}^e$	$E_{\text{rel},B}^e$
<b>1a/1b</b>	1, C <sub>1</sub>	266.8	257.9	248.8
<b>1a/5b</b>	1, C <sub>1</sub>	242.8	233.9	78.4
<b>1b/5a</b>	1, C <sub>1</sub>	248.7	230.7	91.7
<b>1a/5a</b>	1, C <sub>1</sub>	243.3	234.4	86.3
<b>1b/5b</b>	1, C <sub>1</sub>	252.1	234.1	87.7
<b>1a/6d</b>	1, C <sub>1</sub>	385.7	376.8	62.4
<b>1a/8</b>	1, C <sub>1</sub>	221.5	212.6	65.4
<b>1a/10a</b>	1, C <sub>1</sub>	236.1	227.2	140.1
<b>1b/10a</b>	1, C <sub>1</sub>	219.6	201.6	123.6
<b>1a/13c</b>	1 <sup>c</sup> , C <sub>1</sub>	268.8	259.9	89.6
<b>13c/13d</b>	1 <sup>c</sup> , C <sub>1</sub>	188.7	9.5	5.0
<b>2a/2c(s)</b>	1, C <sub>1</sub>	268.8	184.2	187.5
<b>2c/2c(s)</b>	1, C <sub>s</sub>	249.1	167.8	167.8
<b>2c/2c(a)</b>	1, C <sub>2</sub>	350.7	167.8	167.8
<b>2c/2c(b)</b>	1, C <sub>s</sub>	329.8	167.8	167.8
<b>2c/12</b>	1, C <sub>1</sub>	289.1	207.8	7.9
<b>2a/13c</b>	1 <sup>c</sup> , C <sub>1</sub>	296.1	211.5	116.9
<b>2b/13c</b>	1 <sup>c</sup> , C <sub>1</sub>	296.5	207.1	117.3
<b>3a/5b</b>	1, C <sub>1</sub>	303.2	303.2	138.8
<b>3b/5a</b>	1, C <sub>1</sub>	312.1	296.2	155.1
<b>3a/10H</b>	1, C <sub>1</sub>	228.4	228.4	96.0
<b>3a/10C</b>	1, C <sub>1</sub>	270.1	270.1	174.1
<b>4a/5a</b>	1, C <sub>1</sub>	291.1	231.3	134.1
<b>4a/5b</b>	1, C <sub>1</sub>	283.6	223.8	119.2
<b>4a/6b</b>	1, C <sub>s</sub>	431.4	371.6	112.1
<b>4a/8</b>	1, C <sub>1</sub>	241.3	181.5	85.2
<b>5/10</b>	1, C <sub>1</sub>	360.2	203.2	264.2

<sup>a</sup> Full optimizations with 6-31G(d,p) basis set at with respect to **3a** ( $E_{\text{tot}}(\mathbf{3a}) = -721.98656$ ). <sup>b</sup> Geometries given in Figure 6. <sup>c</sup> Energy profiles displayed in Figures 7–9. <sup>d</sup> Characteristics of the electronic structure (1 for singlet and 3 for triplet) and molecular point group. <sup>e</sup>  $E_{\text{rel},3}$  = relative energies with respect to the global minimum **3**;  $E_{\text{rel},A}$  = relative energies with respect to the lower energy minimum; and  $E_{\text{rel},B}$  = relative energies with respect to the higher energy minimum.

**TABLE 3: Total CISD and MCSCF Energies<sup>a</sup>, Electron Configuration, and Coefficients of the Two Most Important Configurations<sup>a</sup> of (CH<sub>4</sub>P<sub>2</sub>) Minimum Geometries<sup>c</sup> 1, 5, 8, 10, 11, and 13**

structure <sup>c</sup>	conf <sup>b</sup> point group	CISD <sup>a</sup> $E_{\text{tot}}$	MCSCF <sup>a</sup> $E_{\text{tot}}$	coeff <sup>b</sup> percent	coeff <sup>b</sup> percent
<b>1a</b>	<sup>1</sup> A, C <sub>2</sub>	-721.973 71	-721.755 25	95	1
<b>3a</b>	<sup>1</sup> A', C <sub>s</sub>	-721.975 31	-721.758 82	93	4
<b>5a</b>	<sup>1</sup> A', C <sub>s</sub>	-721.912 71	-721.698 18	93	3
<b>8</b>	<sup>1</sup> A', C <sub>s</sub>	-721.915 93	-721.699 25	95	1
<b>10a</b>	<sup>1</sup> A', C <sub>s</sub>	-721.939 58	-721.730 31	93	2
<b>10a'</b>	<sup>3</sup> A'' C <sub>s</sub>	-721.939 58	-721.646 03	97	1
<b>11b</b>	<sup>3</sup> A, C <sub>s</sub>	-721.936 41	-721.706 19	97	1
<b>11b'</b>	<sup>1</sup> A, C <sub>1</sub>	-721.936 41	-721.676 99	48	47
<b>13e</b>	<sup>1</sup> A, C <sub>s</sub>	-721.922 40	-721.687 88	49	48
<b>13'</b>	<sup>3</sup> A, C <sub>s</sub>	-721.922 40	-721.689 04	96	1
<b>13f</b>	<sup>1</sup> A', C <sub>2v</sub>	-721.921 20	-721.686 92	49	48

<sup>a</sup> CISD is CISD/6-31G(d,p) reoptimized geometries of the structures in Figure 2. The MCSCF are single points on these CISD geometries and were performed with the software package MOLCAS-4.0<sup>15</sup> using the ANO-S from the MOLCAS basis set library. <sup>b</sup> Electronic states characterized by their symmetry character. Coefficients of the contributing configurations in percent (largest and second largest of 6 configurations listed). <sup>c</sup> For some structures the CISD geometry parameters are included in Figure 2.

NMR shielding, and Wiberg bond index,<sup>16</sup> WBI, and NBO population analysis were carried out using a local version of the GAUSSIAN 98<sup>17</sup> set of programs.

## Results and Discussion

The first part deals with the geometries and the electronic structures of the selected CH<sub>4</sub>P<sub>2</sub> minima **1–14**. How these minima are connected via TS is discussed in the following part.



**TABLE 4: Total MP2/6-31G(d,p) Energies,<sup>a</sup> Zero Point Vibrational Energy,<sup>b</sup> ZPVE, of Optimized Geometries for Defining Bond Dissociation Energies for CH<sub>4</sub>P<sub>2</sub> Isomers**

structure	$E_{\text{tot}}(\text{MP2})^a$	ZPVE
CH <sub>4</sub>	-40.364 63	122.2
PH <sub>3</sub>	-342.578 58	66.2
H <sub>3</sub> C-CH <sub>3</sub>	-79.543 40	203.4 <sup>c</sup>
H <sub>3</sub> C-PH <sub>2</sub>	-381.763 79	148.9 <sup>c</sup>
H <sub>2</sub> P-PH <sub>2</sub>	-683.991 46	97.3
H <sub>2</sub> C=CH <sub>2</sub>	-78.317 28	137.4 <sup>c</sup>
H <sub>2</sub> C=PH	-380.546 37	91.3 <sup>c</sup>
HP=PH	-682.797 26	48.5
H <sup>•</sup>	-0.498 23	0.0
CH <sub>3</sub> <sup>•</sup>	-39.692 70	80.6
H <sub>2</sub> P <sup>•</sup>	-341.953 49	37.2
CH <sub>2</sub> (1)	-38.987 20	45.5
CH <sub>2</sub> <sup>••</sup> (1) <sup>d</sup>	-38.997 92	45.8
CH <sub>2</sub> <sup>••</sup> (3)	-39.019 31	47.7
PH(1)	-341.279 33	15.0
PH <sup>••</sup> (1) <sup>d</sup>	-341.320 58	14.9
PH <sup>••</sup> (3)	-341.342 54	14.8

<sup>a</sup> Energies of unrestricted MP2 also for the closed shell species.<sup>b</sup> ZPVE uMP2/6-31G(d,p)/uMP2/6-31G(d,p) unscaled. <sup>c</sup> In approximate agreement with MP4SDTQ/6-31G(d)/HF/6-31G(d) results<sup>27</sup> for ZPVE in kJ mol<sup>-1</sup>: 187.0 for ethane, 134.7 for Me-PH<sub>2</sub>, 129.3 for ethene, 75.5 for H<sub>2</sub>C=PH, 76.1 for CH<sub>3</sub><sup>•</sup>, and 34.3 for PH<sub>2</sub><sup>•</sup>. <sup>d</sup> A multi configurational treatment would be more appropriate, but was omitted to remain consistent with the general level of theory in this article.

The third part demonstrates the astonishing  $\beta$ -substituent effects on the  $\delta^{31}\text{P}$  NMR signals of the alkyl derivatives of **1a**.

**Equilibrium Structures.** Most of the CH<sub>4</sub>P<sub>2</sub> isomers can be classified into the two groups A and B. Molecules of group A have classical, closed-shell valences (**1–4** in Figure 1). The second group, B, comprises species which can have diradicaloid (or triplet) character like the carbenes (**6**, **7**, and **9**), phosphinidenes (**10**, **11**, and **14**), cyclic betainoid species (**8**, **12**), and PH-CH<sub>2</sub>-PH **13**, the product of homolytic P-P bond cleavage of DPP. Isomer **5** has a special structure which corresponds to the known heteroanalogue PR-P-PR<sup>-</sup> anion<sup>18</sup> and is characterized by the allylic  $4\pi$  electron - 3 center bonding as in the homonuclear allyl anion, C<sub>3</sub>H<sub>5</sub><sup>-</sup>. With few exceptions, the classification by bonding characteristics corresponds to a grouping by relative energies (Figure 3). Similar to phosphirane and its C<sub>2</sub>H<sub>5</sub>P isomers, the CH<sub>4</sub>P<sub>2</sub> structures can be divided into low- and high-energy isomers (with 0 to 100 kJ/mol as low relative energies). The low-energy isomers include **1–4**, and **10**, whereas the high-energy isomers are structures **5–9**, and **11–14**. Although this classification by energy with **10** differing from **11** by 33 kJ/mol is arbitrary, it points to the remarkable relative stability of these phosphinidenes.

The low-energy isomers display similar relative energies and geometries at the different levels of theory employed (e.g., 4.2

(**1a**), 74.8 (**2c**), 0.0 (**3a**), and 51.8 (**4a**) at CISD/6-31G(d,p) with  $E_{\text{tot}}(\text{3a}) = -723.975$  31, see also Table 3). The relative energies of the CH<sub>4</sub>P<sub>2</sub> at B3LYP are about 1% smaller than at MP2 (Table 1). In the following, the geometries and energies of four low-energy isomers from PGs studies<sup>10,11</sup> will be compared with the MP2 results compiled in Table 1 and Figures 2. Thereafter, the CISD and RASSCF results (Table 3) as well as bond energy considerations (Table 4) are presented. The cis-diphosphirane, **1b**, is 9.2 kJ/mol higher in energy than **1a** and its geometry differs from that of trans-diphosphirane merely in the dihedral angle of the cis oriented, exocyclic hydrogen bonds (HPP = 93.7°(trans) **1a**, 96.3°(cis) **1b**). The interconversion of **1a** to **1b** by a phosphorus inversion mechanism, **1a/1b**, has a barrier (258 kJ/mol with respect to **1a**), which is much larger than that for PH<sub>3</sub> or the central phosphorus in CH<sub>3</sub>-PH-PH<sub>2</sub> (at RMP2-(fc)/6-31G(d):<sup>19</sup> 120 kJ, 100 kJ, respectively). The reason for the increase of the barrier is no doubt due to the narrow endocyclic bond angle under the constrain of the small ring. Elongation of the P-C bond opposite to the inversion center,  $P_{\text{inv}}$ , reflects the strain which tends to open up the P-P<sub>inv</sub>-C angle. The electronic structure of the TS **1a/1b** indicates that phosphorus in a trigonal planar coordination is a weaker  $\sigma$  donor than in its pyramidal conformation (the charge of the  $P_{\text{inv}}$ -H group becomes less positive: 0.15 in **1a** to -0.04 in **1a/1b**) and has  $\pi$  donor character toward the CH<sub>2</sub> group (charge of hydrogens attached to C: 0.26 **1a**, 0.20 **1a/1b**). The remarkable, alternative inversion mechanism via a bond breaking - bond making mechanism was first investigated by PG.<sup>11</sup> Although the predicted barriers of 144 to 161 kJ/mol are in reasonable agreement with the refined value of 180 kJ/mol (Table 2), some MNDO transition structures turn out to be either diradical intermediates or to have more than one imaginary vibration mode (see following section on ring opening for details). At all reported theoretical levels (MNDO and methods in Table 1), the diradical mechanism has a lower barrier for the **1a** to **1b** interconversion (e.g., 78 kJ/mol lower at our MP2 level).

However, in **2** the P-C-P bond angles obtained with MNDO differ by less than one degree from MP2 optimized geometries (Figure 2), the P-C double bond is 0.01 up to 0.12 Å longer with MNDO (reported MNDO P-C single bonds in **2a–2d** are between 0.002 Å longer and 0.13 Å shorter than at MP2 level). Nevertheless, the relative MP2 energies of the cis and trans isomers and of the transition structures for the PH<sub>2</sub> group rotation are in rough agreement with previously reported<sup>9</sup> MNDO:  $E_{\text{rel}}(\text{2a with respect to 2c}) = 1$  kJ/mol MNDO, 3.2 kJ/mol at MP2; the largest rotation barrier is 12.2 kJ/mol at MNDO and 13.6 kJ/mol at MP2. The small barriers of rotation around the C-PH<sub>2</sub> bond indicate, that detection of distinguishable rotamers is not an intrinsic property of the P=C-P framework but probably due to substituent and solvent effects.

**TABLE 5: NMR Chemical Shifts of <sup>31</sup>P,  $\delta^{31}\text{P}$ , Calculated<sup>a</sup> Geometries Together with Characteristic Electronic<sup>b</sup> and Geometric Parameters<sup>c</sup> of Cyclo-(CR<sub>2</sub>)(PR')<sub>2</sub> with R (on Carbon), R' (on Phosphorus) = H and/or C'H<sub>3</sub>**

R	R'	$\delta^{31}\text{P}$	$\delta'^{31}\text{P}$	q(P) <sup>b</sup>	q'(P) <sup>b</sup>	$\Sigma\alpha^c$	PP	PC	PPC	R'PP	R'PC
H	H	-267	-301	0.11	0.27	243.5	2.235	1.871	53.3	94.1	96.1
H	C'H <sub>3</sub>	-188	-237	0.33	0.48	254.4	2.222	1.870	53.5	100.3	100.6
C'H <sub>3</sub>	H	-182	-228	0.08	0.28	244.6	2.236	1.885	53.6	94.3	96.7
(C'H <sub>3</sub> ) <sup>d</sup>	H	-263	-299	0.11	0.27	- <sup>d</sup>	2.236	1.885	<i>d</i>	<i>d</i>	<i>d</i>
C'H <sub>3</sub>	C'H <sub>3</sub>	-111		0.34	0.49	261.9	2.224	1.890	54.0	102.5	105.4

<sup>a</sup> Although  $\delta^{31}\text{P}$  was calculated at GIAO/B3LYP/6-311G(d) on B3LYP/6-31G(d), the  $\delta'^{31}\text{P}$  (GIAO/MP2/6-31G(d,p)/MP2/6-31G(d,p) calculations could not be done for (CH<sub>3</sub>)<sub>2</sub>C(P-CH<sub>3</sub>)<sub>2</sub>; For transformation from shieldings to chemical shifts the theoretical reference PH<sub>3</sub> was used:  $\delta^{31}\text{P}(\text{PH}_3, 1) = -240$ ; magnetic shielding of <sup>31</sup>P at GIAO/B3LYP/6-311G(d)/MP2(fc)/6-31G(d,p) = 561.1 ppm and at GIAO/MP2/6-31G(d,p)/MP2/6-31G(d,p) is 643.1 ppm. <sup>b</sup> The q(P) are Mulliken atomic charge and the q'(P) are NPA<sup>34</sup> charges at phosphorus computed at the B3LYP level of the NMR calculations. <sup>c</sup> Bond angle sum,  $\Sigma\alpha$ , is the sum of the angles P-P-C, R'-P-P, and R'-P-C in degree. <sup>d</sup> In the optimized structure of cyclo-(C(CH<sub>3</sub>)<sub>2</sub>)(PH)<sub>2</sub> the CH<sub>3</sub> groups are replaced by hydrogen and only the C-H parameters are reoptimized.

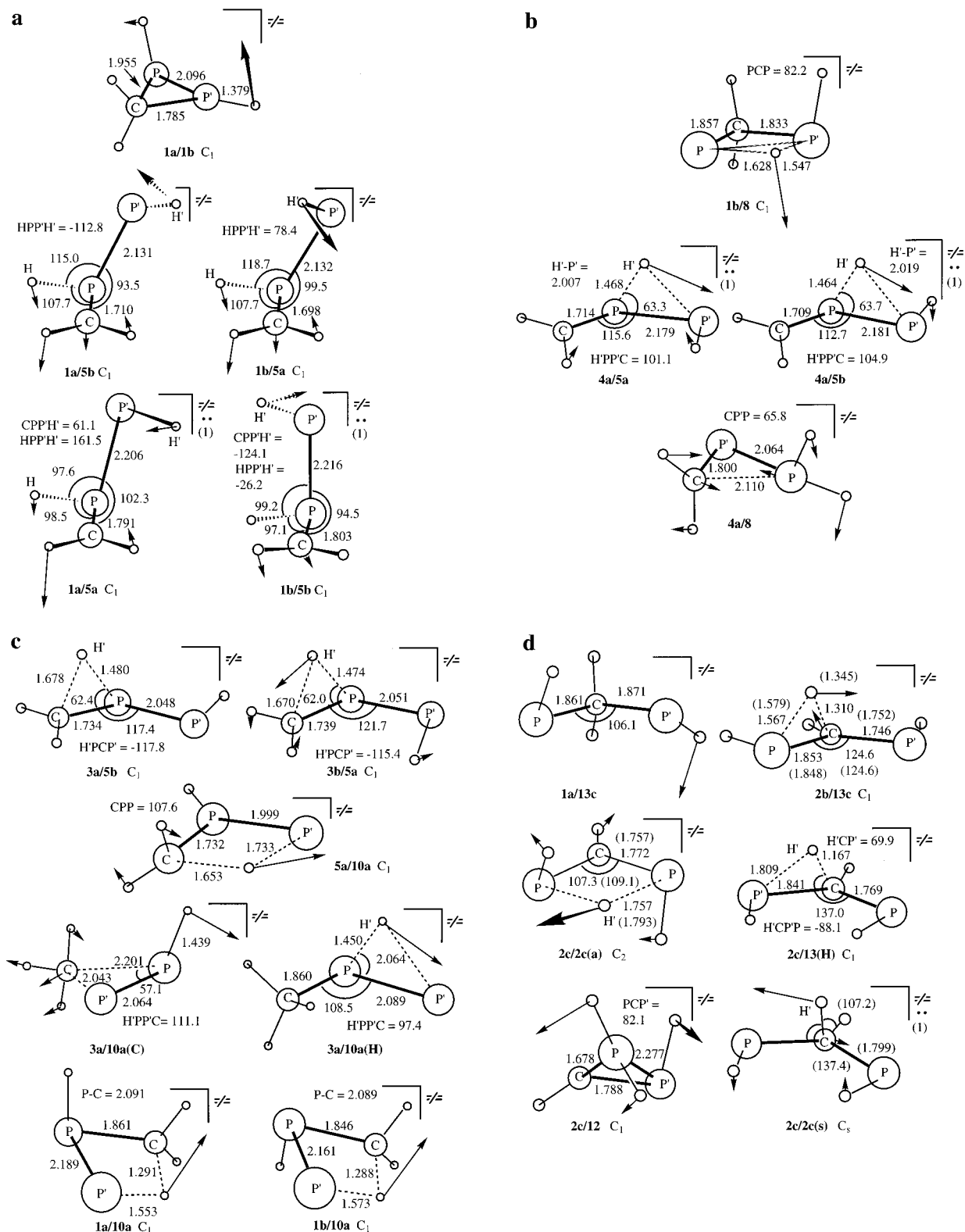


**Figure 6.** Geometries (bond length in Å; angles in degree) of  $\text{CH}_4\text{P}_2$  isomer transition structures, TS (CISD/6-31G(d,p) parameters in parentheses).

Methyldiphosphene, **3**, is the simplest methyl derivative of diphosphene but due to the lack of protecting groups, it is too reactive to be easily obtained experimentally.<sup>20</sup> Probably because of the “double bond rule”,<sup>21</sup> which declared the orbital overlap of post first row elements to be too small to form stable  $\pi$  bonds, this molecule was neglected in previous DPP studies. Nevertheless, methyldiphosphene is not only another example refuting

this “rule” but also the global minimum structure on the  $\text{CH}_4\text{P}_2$  energy hypersurface. The MP2 geometries have slightly longer P–P bond length than in a previous RHF/dz2p study.<sup>12</sup> In agreement with the previous RHF study,<sup>12</sup> the methyl group has little effect on the HPP angle because the electronegativity difference between carbon and phosphorus is small ( $\text{EN}(\text{C}) = 2.5$ ,  $\text{EN}(\text{P}) = 2.1$ ) and contribution of the  $\text{X}^-(\text{P}_2\text{H})^+$  resonance

structure is negligible. Although there is only one  $\text{CH}_4\text{P}_2$  isomer with a P–P double bond, **3**, there are two isomers with a P–C double bond: **2** (see above) and **4**.

The 1,2-diphospha-2-propene, **4**, with a P–P single and two C–H bonds is 59.8 kJ/mol higher in energy than **3** but about 20 kJ/mol more stable than **2**, which has a P–C single, one P–H and one C–H bond. Because a P–P single bond can be expected to have a smaller bond strength than a P–C single bond, the stability of **4** over **2** may be due to delocalization in the  $\text{P}_2\text{C}$  framework. A rotation of the phosphino group was calculated to have an energy barrier of 16.5 kJ/mol via TS **4/4**. This is less than 3 kJ/mol higher than the corresponding barrier in **2** and does not appear to explain a 20 kJ/mol stabilization of **4** over **2**. The P–C double bond length in **4** (1.677 Å) is about as long as in the parent  $\text{HP}=\text{CH}_2$  (1.676 Å) and shorter than in the conformers of **2** (1.683 to 1.686 Å). Therefore, stabilization of **4** is likely to be due to stronger P–C  $\pi$  bonding.

The phosphinidene **10** is the fifth low energy  $\text{CH}_4\text{P}_2$  isomer. It has not only a remarkable low energy (e.g., 14.7 kJ/mol relative to **2** the precursor of several DPP derivatives) but also has the planar tricoordinate phosphorus known from previous studies of phosphinophosphinidenes.<sup>22</sup> Comparing the geometric parameters of the phosphinophosphinidenes  $\text{P}-\text{HP}-\text{EH}_n$ , with  $\text{EH}_n = \text{H}$ ,  $\text{CH}_3$ ,  $\text{Cl}$ , and  $\text{F}$  confirms that the substituent  $\text{EH}_n$  has little effect on the P–P bond length in the triplet but shortens P–P with increasing electronegativity of E (the P–P in Å of the singlet  $\text{P}-\text{HP}-\text{EH}_n$  at MP2 is 1.947 (H), 1.946 ( $\text{CH}_3$ ), 1.918 (Cl), and 1.905 (F); at CISD/6-31G(d,p) is 1.951 (H), 1.943 ( $\text{CH}_3$ ), 1.916 (Cl), and 1.898 for  $\text{EH}_n = \text{F}$ ). This relationship is in agreement with the MO picture in Figure 4. In the singlet the  $p_{\pi,x}$  AO at phosphinidene P is occupied together with the P–P  $\pi$  bond ( $\pi_x^2$ ,  $(P - P' - \pi_y)^2$ ). The strength of the  $P - P' - \pi_y$  bond depends on the  $\pi_y$  donor strength of  $\sigma^3\text{-P}$ . The  $\pi$  donor character of the  $\text{Lp}(\sigma^3\text{-P})$  increases with its p-character. Enforced planarization of  $\sigma^3\text{-P}$  gives rise to a high p-character and  $\pi$  donor strength.<sup>23</sup>

Another way of increasing the donor strength is based on the  $\sigma$  acceptor effect of chlorine or fluorine toward phosphorus which reduces the s-character of the  $\text{Lp}(\sigma^3\text{-P})$  and increases its p-character. In the triplet **10b** and the diradical **10c**, the  $\text{Lp}$  on  $\sigma^3\text{-P}$  and both  $p_\pi$  AO at phosphinidene P are singly occupied ( $\pi_x^1$ ,  $\pi_y^1$ ,  $\text{Lp}(P')^2$ ; Figure 4). The diradical has a similar geometry as the triplet. The trend of the relative singlet energies with respect to the triplet,  $\Delta_{S,T}E$ , in the set of  $\text{P}-\text{HP}-\text{EH}_n$  molecules is the same at MP2 ( $\Delta_{S,T}E$ : 15 (H), –8 ( $\text{CH}_3$ ), –20 (Cl), and –38 for  $\text{EH}_n = \text{F}$ ) and at CISD/6-31G(d,p) ( $\Delta_{S,T}E$ : 45 (H), 32 ( $\text{CH}_3$ ), 30 (Cl), and 14 for  $\text{EH}_n = \text{F}$ ) and is in agreement with the results of the previous QCISD/6-311G(d,p)//MP2/6-31G(d,p) study<sup>24</sup> ( $\Delta_{S,T}E$ : 28 (H), 5 (Cl), and –20 for  $\text{EH}_n = \text{F}$ ). Increasing relative stability of the singlet phosphinidene is related to the increased electronegativity of the  $\text{EH}_n$  substituent. In this context, the  $\beta$  substituent methyl displays a similar stabilization on singlet phosphinidene as chlorine. This observation is consistent with a study<sup>13</sup> on the heteroanalogue  $\text{H}-\text{C}-\text{PH}-\text{EH}_n$  carbenes, which shows that a methyl group tends to reinforce the stabilizing contribution of a phosphino group on a singlet carbene compared to  $\text{EH}_n = \text{H}$  in the parent phosphinocarbene. Because of the proximity of singlet and triplet **10** is probably the most reactive species of the low energy isomers.

The two high-energy isomers **8** and **11** only differ by one P–P bond. The acyclic **11** is 16.8 kJ/mol more stable than the cyclic isomer, **8**. Because of the lack of a  $\pi$  donor substituent, the phosphinidene **11** only exists as triplet (the singlet of

structure **11** has no barrier toward **8**). The formal description of **8** as a betain is not justified by the electron distribution obtained from ab initio MO calculations (group charges: –0.05 P, 0.02  $\text{CH}_2$ , and 0.03  $\text{PH}_2$ ). Nevertheless, the bond orders indicate a Lewis structure (WBI: 1.02 C– $\text{PH}_2$ , 0.926 C–P, and 1.088 for the P–P bond). The contradiction of the two previous sentences is abrogated by a look at the highest MOs of **8** (Figure 5). Considering **8** to be held together by a combination of the orbitals of a  $\text{CH}_2 = \text{PH}_2^+$  cation and a  $\text{P}^-$  anion, the four highest energy MOs can be used to explain the transannular bonding (sigma aromaticity,<sup>25</sup> respectively) of the three-membered ring. Although the HOMO, the 20th occupied MO, is mainly a phosphorus lone pair ( $p_{\pi,z}(\text{P}^-)$ ), the MO's 19, 18, and 17 illustrate how the ring bonds are composed. In Figure 5, the  $\text{CH}_2 = \text{PH}_2$  bond lies in  $x$  direction, the  $y$  axis orthogonal to  $x$  and in the ring plane, and the  $z$  axis is orthogonal to the ring plane. MO 19 is a combination of  $3p_y(\text{P}^-)$  with the  $\pi_y$  bond of the  $\text{CH}_2 = \text{PH}_2^+$  fragment. In MO 18, the  $3p_x(\text{P}^-)$  combines with the empty  $\pi_y^*(\text{CH}_2 = \text{PH}_2^+)$  fragment orbital. As in MO 19, the centroid of orbital overlap is inside the ring in MO 17. Furthermore, in MO 19 as well as in 17 the  $3p_y(\text{P}^-)$  fragment orbital is involved. However, in MO 19  $3p_y(\text{P}^-)$  interacts with a  $\pi$  bond, it merges with the  $\sigma_x^*(\text{CH}_2 = \text{PH}_2^+)$  in MO 17. Consequently, depopulating MO 18 (e.g., in the triplet) weakens the P– $\text{PH}_2$  bond and leads to ring opening.

Similar to **8** and **11**, the triplet of **13** has no cyclic pendant (triplet of **1** has no barrier to ring opening by P–P bond cleavage). Nevertheless, some of the triplet state minimum conformations **13a–13d**, have corresponding diradical minima (**13e**, **13f**, Figure 2). The diradical **13e** and its enantiomer represent the primary products of homolytic P–P bond cleavage in **1**. In contrast to the MNDO based study by PG in 1994,<sup>11</sup> the structure with both P–H bonds eclipsed ( $\tau = 0$  degree, Figure 2) is neither a minimum nor a TS (neither for the singlets nor the triplet state) at MP2 level. The triplet minima **13a** and **13b** have no corresponding diradical structures (Diradicals with structure of triplet **13a** or **13b** have no barrier toward **1a**, **1b** respectively). The diradical minimum, **13e**, can transform to **1a** or **1b** by “rotation” of the PH group, whereas **13f** has to pass **13e** or its enantiomer to isomerize to **1**. The barriers for interconversion of the conformers of **13** and for isomerization are discussed in the following section about TS. Because of the central  $\text{CH}_2$  group (providing no  $\pi$  group orbital required for a delocalized  $\pi$  bonding as in **5**), structures **13a–13d** are not stabilized by  $\pi$  conjugation.

Although the relative energy of acyclic  $\text{CH}_2\text{--PH--PH}$ , **5**, is similar to that of cyclic **8**, their electronic structure differs distinctly. The isomers **5a** and **5b** have a typical allyl conjugation with a 4  $\pi$  electron system delocalized over the three atoms C, P and  $\text{P}'$  (2). Bond length as well as WBI indicate the P–P as well as the P–C bond to be between single and double bonds (as to be expected for allyl conjugation). Despite the P–P bond is only a partial double bond, the allyl conjugation enforces the substituents in the  $\text{CP}_2$  plane. With three different substituents on the planar  $\sigma^3\text{-P}$ , the two conformers, **5a** and **5b** are minima. Remarkably, the  $\text{H}-\text{P}'-\text{P}$  angle in **5b** is even smaller (87.4°) than in the planar cation  $\text{H}_2\text{P}-\text{PH}^+$  (89.5°). The triplet  $\text{CH}_2\text{--PH--PH}$ , **5c**, does not gain stabilization from allyl delocalization. It has a normal trigonal pyramidal  $\sigma^3\text{-P}$ , and is 75 kJ/mol higher in energy than **5a**. In contrast to delocalization in **5c**, localization of charges is strongest in the betainoid structure **14**.

Although  $\text{PH}_2$  appears as a ring fragment,  $\text{PH}_3$  does not (although pentacoordinate phosphorus is known). Isomers **9** and **14** are acyclic structures with the  $\text{PH}_3$  group as a moderate a



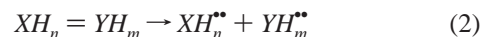
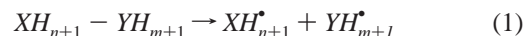
electron donor. The group charge of the “PH<sub>3</sub><sup>+</sup>” group is 0.67 in **14** and 0.33 in **9** (Mulliken; 0.72 and 0.73 with NBO, respectively). In **9**, the short HP–C bond length and the negative atomic charge on carbon (−0.37 in **9a**, −0.31 in **9b**, Mulliken; −1.07 and −1.06 with NBO, respectively) are indicators for the PH group acting as a  $\pi$  donor stabilizing the singlet carbene. The triplet **9c** is 34.2 kJ/mol higher in energy than **9a**. Because **14** can be considered as primary adducts of PH<sub>3</sub> to H–CP, the dissociation barrier,  $\Delta_{\text{Diss}}E$ , of this structure was evaluated. The  $\Delta_{\text{Diss}}E(\mathbf{14} \rightarrow \text{PH}_3 + \text{H–CP})$  of 6 kJ/mol characterizes **14** as kinetically instable. Isomer **12** is about as instable as **14**. Nevertheless, **12** does not decompose but transforms to **2** by ring opening (P–P bond cleavage). The formal description as a betain, molecular dipole, is not fully justified based on the ab initio charge distribution. The CH fragment has a group charge of −0.28 (Mulliken; −0.87 NBO) and the compensating positive charge is mainly at PH<sub>2</sub>. The P–P bond is the weakest of the endocyclic bonds (WBI = 0.96) and the PH<sub>2</sub>–CH<sub>2</sub> is the strongest (WBI = 1.27). Similarly to **8**, the MO's can be build up from a CH<sup>−</sup> and a PH–PH<sub>2</sub><sup>+</sup> moiety.

The highest energy isomer considered is the carbene **7**. In contrast to PH=C–PH<sub>3</sub>, **9**, PH<sub>2</sub>–C–PH<sub>2</sub>, **7**, could form an allyl conjugate electronic structure like PH<sub>2</sub>–PH–CH<sub>2</sub>, **5**. However, only one inherently pyramidal  $\sigma^3$ -P has to be planarized in **5**, the phosphorus inversion barrier would have to be overcome twice to form a 4  $\pi$  electron allyl system in **7**. An alternative to the three center delocalization is formation of one double bond (PH<sub>2</sub><sup>(+)</sup>=C<sup>(−)</sup>–PH<sub>2</sub>) similar to that in **9**. Geometries **7a** (C<sub>s</sub>) and **7b** (C<sub>2</sub>) represent a compromise, pyramidal of both  $\sigma^3$ -P is considerably reduced and the P–C bond length shrinks to 1.67 Å (compared to 1.86 in Me–PH<sub>2</sub>). This partial  $\pi$  conjugation is also reflected by the WBI of 1.53 **7a** and 1.54 **7b**, characterizing the P–C bonds as half double bond. Although **7a** and **7b** are minima at CISD/6-31G(d,p), these structures are shallow TS at MP2/6-31G(d,p). In both conformations, the triplet carbene is less stable than the singlet (Table 1). This singlet stabilization is in agreement with previous investigations on PH<sub>2</sub>–CH and PH<sub>2</sub>–C–CH<sub>3</sub> with one  $\sigma^3$ -P  $\pi$  donor. **7a** and **7b** are also connected through TS **7a/7b** in which rotation of both phosphino groups occurs, with a barrier height of 44 kJ/mol, relative to **7b**. Although the inversion mechanism via a (PH<sub>2</sub><sup>(+)</sup>=C<sup>(−)</sup>–PH<sub>2</sub>) structure is probably preferred over rotation in **7**, for **1** the inversion is circumvented by an alternative mechanism. This shows that there may be more than one way from A to B on the hypersurface of CH<sub>4</sub>P<sub>2</sub>.

The multiconfigurational character of some CH<sub>4</sub>P<sub>2</sub> isomers is considered by reoptimizing at CISD/6-31G(d,p) and single point calculations at MC-SCF level on these geometries (Table 3). Although most of the selected isomers do not require MCSCF treatment, the results for **10** and **13** are noteworthy. The structure of CH<sub>3</sub>–PH–P with a planar tricoordinate phosphorus, **10a**, is confirmed to be a closed-shell singlet minimum. Nevertheless, the triplet minimum with pyramidally coordinate phosphorus is 32 kJ mol<sup>−1</sup> lower in energy. For **13**, the intermediate of direct ring opening of **1a**, a MCSCF treatment is obviously appropriate: The coefficients of the <sup>1</sup>A<sub>1</sub> state are 48% (b<sup>1</sup> occ., a<sup>2</sup> empty), 49% (b<sup>1</sup> empty, a<sup>2</sup> occ), and 3% other configurations). The <sup>1</sup>B<sub>1</sub> and <sup>1</sup>A<sub>2</sub> are also mostly two configuration cases, while in the <sup>1</sup>B<sub>2</sub> state one configuration has 93% (approximately closed shell).

With an appropriate set of bond energies, the relative energies of isomers can be estimated.<sup>26</sup> Although a plethora of somehow defined “bond energies”, BE, exists,<sup>3</sup> the bond separation energy,

BSE,<sup>27,28,29</sup> is probably the most straightforward definition of a BE (eq 1 and 2, with X = C and Y = P and  $n = 2$  and  $m = 1$ ).



Unfortunately, no consistent set of BE for all bonds in the CH<sub>4</sub>P<sub>2</sub> isomers is available (bond enthalpies<sup>3</sup> only 321 (P–H), 264 (P–C), and 200 for P–P;  $\sigma$ -bond strength<sup>30</sup> 368 (C–C), 255 (P–P);  $\pi$ -bond strength<sup>31</sup> 293 (C=C), 201 (C=P), 143 (P=P); all energies in kJ mol<sup>−1</sup>). Therefore, the required BSEs have been recalculated at the theoretical level of this study, MP2/6-31G(d,p). The total and zero point vibration energies of the molecules and “fragments” (required in eq 1 and 2) listed in Table 4 give BSE in kJ mol<sup>−1</sup>: 372 for C–C, 278 for C–P, 199 for P–P, 304 for P–H, and 414 for C–H, whereas the ranges are 690–854 for C=C, 456–704 for C=P, and 275–608 for P=P (the lower BSE consider the triplet “fragments”). Because of the ambiguity of the “fragments” (singlet, diradical, or triplet) these BSE are not well quantified. Nevertheless, for the estimation of  $E_{\text{rel}}$ , of the CH<sub>4</sub>P isomers below, the BSE reaction to the triplet “fragments” are used to calculate the atomization energies, EA, (EA =  $\Sigma$ BSE;  $E_{\text{rel,est}}(\mathbf{i}) = \text{EA}(\mathbf{1}) - \text{EA}(\mathbf{i})$  with EA(**1**) = EA(**8**) = 2191 kJ mol<sup>−1</sup>). Though most  $E_{\text{rel,est}}(\mathbf{i})$  deviate considerably from the ab initio  $E_{\text{rel}}(\mathbf{i})$ , some isomers show outstanding differences: (a) the  $E_{\text{rel,est}}(\mathbf{i})$  of **3** is overestimated by 92 kJ mol<sup>−1</sup>; (b) the  $E_{\text{rel,est}}(\mathbf{i})$  of the allyl conjugate **5** is estimated 121 kJ mol<sup>−1</sup> too high due to considering one C–P and one P–P single bond for this isomer; (b) for the cyclic isomers **8** and **12**  $E_{\text{rel,est}}(\mathbf{i})$  are only zero and 110 kJ mol<sup>−1</sup> due to the neglect of ring strain. The two lowest energy isomers, **1** and **3**, differ by the following (change from **1** to **3**): −1 P–H, +1 C–H, −1 C–P, and P–P changes to P=P. The change of A–H bond should be in favor of **1** by 110 kJ mol<sup>−1</sup>. Furthermore, the lack of one C–P bond (BSE = 199) should make **1** more stable. The extra  $\pi$  bonding in **4** approximated from the difference of BSE(P–P) to BSE(P=P, triplets) of 76 kJ mol<sup>−1</sup> only partially compensates the 309 kJ mol<sup>−1</sup> from the other bond changes. The large discrepancy with respect to the explicit calculated  $E_{\text{rel}}$  demonstrates the drawbacks of the bond energy concept. Interestingly, the relative energies of **2** and **4** are overestimated by about the same amount (−50 and −40 kJ mol<sup>−1</sup>, respectively).

**Transition Structures.** Searching for transition structures, TS, on an energy hypersurface, EHS, is guided by the quest for alternative pathways to interesting products and their kinetic stability. Neglect of solvent effects is reasonable for rearrangements of neutral molecules and homolytic cleavage. An investigation of heterolytic diphosphirane, DPP, reactions including ionic reaction pathways will be the subject of a special article considering “solvent effects on base induced diphosphirane ring opening”. The following discussion is based on the MP2/6-31G(d,p) structures (Figure 6) and relative energies (Table 2) of the TS which were located on the EHS of CH<sub>4</sub>P<sub>2</sub> (Figures 7, 8, and 9). Despite DPP, **1**, is not the global CH<sub>4</sub>P<sub>2</sub> minimum, the ring opening reactions of **1** are discussed first. The acyclic structures with C–P–P (Figure 7, 8) and P–C–P backbone (Figure 9) can interconvert via cyclic intermediates or by migration of a CH<sub>n</sub> group (e.g., CH<sub>3</sub> in **4/10aC**). Reactions of the cyclic **1** tautomers, **8** and **12**, are included in the second and third section about rearrangements of C–P–P and P–C–P backbone species, respectively. At last, the CH<sub>3</sub> migration in



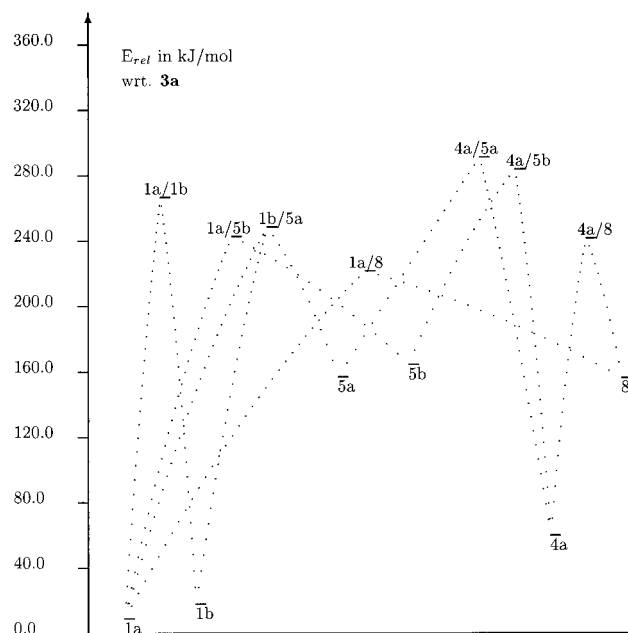


**Figure 7.** Energy diagram of  $\text{CH}_4\text{P}_2$  minimum and transition structures with C-P-P backbone (first set;  $E_{rel}$  in kJ/mol).

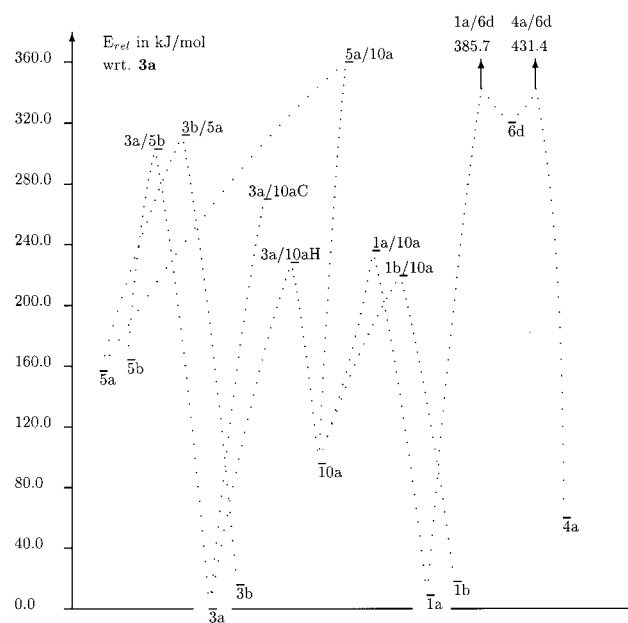


**Figure 8.** Energy diagram of  $\text{CH}_4\text{P}_2$  minimum and transition structures with C-P-P backbone (second set;  $E_{rel}$  in kJ/mol).

**4/10C** is compared with the hydrogen shift in the TS **4/10H** and the homolytic rupture of endocyclic bonds is briefly discussed.

In contrast to phosphirane, with a hydrogen shift assisted ring opening having the lowest barrier for breaking an endocyclic bond, no corresponding TS exists for **1**. This is due to the ability of the PH group (but not the  $\text{CH}_2$  group) to participate in an allyl conjugation. Shifting  $\text{H}'$  in the  $\text{X-CHH}'\text{-P'H}$  ring (with  $\text{X} = \text{CH}_2$  in phosphirane;  $\text{X} = \text{PH}$  in **1**) leads to one double bond in phosphapropene for  $\text{X} = \text{CH}_2$  because the  $\text{H}'$  bridged  $\text{P}'\text{-C}$  bond does neither open to the instable  $\text{PH}_2\text{-CH}_2\text{-CH}$  nor transforms to the hypothetical cyclic ylid, cyclo- $(\text{CH}_2)(\text{CH})\text{-(PH}_2)$ . Even though the cyclic  $\text{CH}_4\text{P}_2$  ylid **12** is a minimum, the corresponding shift of  $\text{H}'$  (with  $\text{X} = \text{PH}$ ) in **1** does not lead to this energy rich structure ( $E_{rel} = 281$  kJ/mol). Furthermore, the P-X endocyclic bond is much less polarized in **1** ( $\text{X} =$

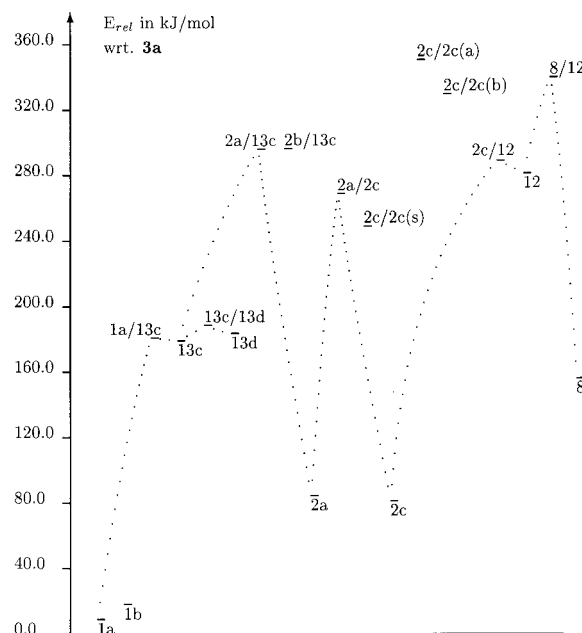


**Figure 9.** Energy diagram of  $\text{CH}_4\text{P}_2$  minimum and transition structures with P-C-P backbone ( $E_{rel}$  in kJ/mol).

PH) than in phosphirane ( $\text{X} = \text{CH}_2$ ) and, therefore, less easily broken. Consequently, breaking the  $\text{H}'$  bridged  $\text{P}'\text{-C}$  bond while trying to shift  $\text{H}'$  in **1** from C to  $\text{P}'$  is the preferred process with a barrier around 230 kJ/mol (**1/5** TSs are pure P-C cleavages Figure 7; combined  $\text{H}'$  shift and cleavage TS **1/6** in Figure 8 with barrier of 386 kJ/mol with respect to **1**). Without hydrogen shifting, the allyl conjugate **5** can close the ring toward **1**. The barriers for conrotatory ring opening (**1a/5b**, **1b/5a** Figure 7) are similar to those of the disrotatory process (**1a/5a**, **1b/5b**). Because the conrotatory TS have diradical character, the MP2 barriers are unprecise. The diradical character of the transition structures in Figure 6 with 1,2 hydrogen shift is negligible.

The lowest barrier for a reaction of **1** is 212.6 kJ/mol high and represents the tautomerization of **1** via **1/8** to **8** (Figure 7). The  $(\text{CH})(\text{PH})(\text{PH}_2)$  ring is only formally an ylide (see previous section) and is connected to the acyclic structure **4** by a barrier of only 80 kJ/mol. A fourth alternative reaction of **1** leads to the phosphinidene **10** and has an intermediate barrier height (e.g., **1a/10a** with respect to **1a** is 225, which is an *upper limit estimate* because stabilizing open shell contributions are underestimated at MP2). Once **10** is formed, it may ( $E_{rel,10}(\text{3/10aH}) = 228.4$  kJ/mol) rearrange to **3**. Despite the intermediate, **8**, of the lowest energy pathway for opening **1** appears unusual for a small ring, tetracoordinate phosphorus is normal in larger rings.

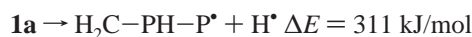
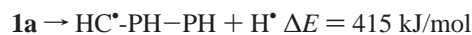
Only in the fifth pathway of opening the **1** ring leads to a structure with a P-C-P backbone; the P-P bond is homolytically broken and the intermediate diradical or triplet can convert to 1,3-diphosphapropene by hydrogen migration from C to P. The rearrangement has a barrier of 296 kJ/mol, which is more than 60 kJ/mol higher than the TS leading to structures with C-P-P backbone. In conclusion, opening **1** toward C-P-P backbone species has smaller energy barriers than that toward other products. Nevertheless, these barriers provide **1** with a sufficient kinetic stability. Slightly higher barriers (228.4 and 303.2 compared to 212.6 kJ/mol, Table 2) give kinetic stability to the global minimum **3**. Although the isomerizations of C-P-P based structures are discussed in the following, the question of how the experimentally known molecules with P-C-P backbone are related to **1** is addressed in a later section.

The C–P–P backbone hampers highly symmetric transition structures. Although the 1,3-H shift TSs in this section all comprise an asymmetric P–H–C bridge, the 1,2-H shift TSs are either migrations over a single bond (**3/5**), over a localized  $\pi$  bond (**3/10H**), or over a delocalized  $\pi$  system (**4/5**). The energies of these 1,2-H shift TSs with respect to their educts (lowest energy minimum connected to the TS) are 300, 230, and 220 kJ/mol, respectively. This order reflects the support of a  $\pi$  system for 1,2 migration. The TS of **4** are of special interest because derivatives of 1,2-diphosphapropene-2 are frequently used in the synthesis of DPP derivatives. Therefore, the second TS of **4**, **4a/8** (Figures 6 and 7), which does not only open another path to **1** but is also 40 kJ/mol lower than **4a/5**, is noteworthy. In TS **4a/8**, the C–P(H<sub>2</sub>) bond is already elongated by 0.3 Å (relative to **8**), and the conrotatory character of this TS becomes clear when looking at the transition trajectory in Figure 7. On the way to **1**, **8** passes **1b/8** ( $E_{\text{rel},s}(\mathbf{1b/8}) = 212.8$  kJ/mol), which is a TS of different character: the P–P bond is hydrogen bridged and temporarily widened by 0.6 Å (with respect to **8**). Other hydrogen bridged TS are **1/10** (discussed before) and **5/10**. In contrast to **1a/10** or **1b/10** with the remaining PH group pyramidal coordinate, the corresponding PH moiety is approximately planar in **5/10** (Figure 8). Furthermore, the shifting hydrogen moves in the plane of the heavy atoms in **5/10** (H moves through or over the PC<sub>2</sub> plane in **1a/10** and **1b/10**, respectively) with about equal distances to the bridgehead atoms, C and P. The P–P double bond of the singlet phosphinophosphinidene **10**, is almost formed in **5/10** giving this TS the character of an H exchange between a carbanion Lp<sub>x</sub> and a phosphinidene Lp<sub>x</sub> (both Lp<sub>x</sub> in *xz* plane; Figure 4). An 1,2-H shift TS where the hydrogen is not bridging but only supports the rearrangement, is **1/6**.

The P–C–P backbone isomers of CH<sub>4</sub>P<sub>2</sub> could transform via high symmetric TS. Nevertheless, only the TS **2c/2c(a)** has a 2-fold axis. Most isomerizations of P–C–P backbone species lead to minima with a small singlet/triplet gap, so that the TS also have partial open shell character. The symmetric opening of **1** toward **13**, is obviously a homolytic cleavage of the P–P bond resulting in a diradical structure. The diradical singlet, as well as the triplet, of PH–CH<sub>2</sub>–PH form symmetric minima (*anti*: H–P–C–P = 180°, **13f**, **13d**, Figure 2), which can rotate to a less symmetric minimum via TS **13c/13d** (Figure 6). Rotating both PH groups out of the anti conformation does not lead to a stable singlet but to closure of the P–P bond together with the loss of the open shell electron configuration. Therefore, the character of a PH rotation dominates over the ring closure in the TS **1a/13c**. A distinctly different character is found for the transition of **13** toward an acyclic product, **2a/13** ( $E_{\text{rel},3} = 304.2$  kJ/mol; Figure 9). Besides the open shell character of the structures involved, this transition process resembles the characteristics of an 1,2-H shift over a  $\pi$  system (substituents on P'–C about coplanar, H' above this plane with P'–H' and C–H' equally elongated by about 0.2 Å). The inaccuracy of the MP2 treatment for  $E_{\text{rel}}(\mathbf{2b/13c})$  may be estimated by looking at the relative energy of the triplet energy for this structure ( $E_{\text{rel}}(\text{triplet/singlet}, \mathbf{2a/13c}) = 90$  kJ/mol). Once the ring **1** is opened toward **2** with a P–C–P backbone, tautomerization can only lead to the high energy isomers **7**, **9**, **11**, and **13** and ring closure can transform **2** to **12**. Although the tautomerizations are neglected here due to their high barriers, the ring closing via **2c/12** to a cyclic tautomer of **1** with a reaction barrier of 207.8 kJ/mol is considered (Figure 6). Nevertheless, the product of this ring closure, **12**, is only an temporary structure in a further isomerization to the second lowest energy cyclic diphosphirane

tautomer (**8** via **8/12**) because the barrier of **12** toward reopening is only 7.9 kJ/mol. In conclusion, the kinetic stability of the experimentally known derivatives of **2** is probably due to the high barriers of the intramolecular rearrangements. For chiral derivatives of **2**, R'R''P–CR=PR', mixing of the primed substituents via one of the **2/2** TSs competes with the ring closure to the corresponding DPP.

The hydrogen shift, **3a/10a(H)**, is preferred over the methyl migration, **3a/10a(C)**, by about 42 kJ/mol for isomerization between the methyldiphosphene, **3** and the phosphinidene **10**. Although hydrogen migration can use a bridged TS with efficient three-center conjugation, the more electronegative carbon tends to withdraw electrons from the P–P moiety. This difference in polarization in **3a/10a(H)** and **3a/10a(C)** is reflected by the P–P–X angle (with X = H in **3a/10a(H)**, X = CH<sub>3</sub> in **3a/10a(C)**), which is smaller (106.8°) in **3a/10a(H)** than in **3a/10a(C)** with 108.5°. Considering the generation of a radical CH<sub>3</sub>P intermediate by cleavage by a P–H versus a C–H bond provides an interesting result:



As the synthesis of **1** by carbene addition to HP=PH, the P–H and C–H cleavage have no reaction barrier (the dissociation product has highest energy on reaction path). The P–H bond dissociation energy in **1a** of 311 kJ/mol is comparable to the corresponding value of 321 kJ/mol for phosphirane.<sup>13</sup>

Thus, a homolytic P–H bond cleavage is about 100 kJ/mol more facile than a C–H rupture for diphosphirane. This  $\Delta E$  difference seems to be large enough to rule out a participation of a C–H bond rupture, in a homolytic dissociation–association rearrangement of diphosphirane.

**<sup>31</sup>P NMR Chemical Shifts.** The analytic tool of nuclear magnetic resonance, NMR, can often be supported by computed predictions where experimentally investigated molecules are small or effects of remote substituents are negligible or estimated. Table 5 demonstrates that  $\beta$  substituent effects on phosphorus can be of the same amount as the  $\alpha$  substituent effects; the chemical shift,  $\delta^{31}\text{P}$ , of the **1a** derivative with methyl substituents on phosphorus, –188 ppm, is almost the same as with methyl on the carbon ring fragment, –182 ppm at B3LYP/6-311G(d)//B3LYP/6-31G(d). Including electron correlation in GIAO/MP2/6-31G(d,p)//RMP2/6-31G(d,p) reduces the  $\alpha$ - (64 ppm downfield) as well as the  $\beta$ -substituent effect (73 ppm) without changing the trend ( $\beta$ - slightly stronger than  $\alpha$ -effect). These coinciding chemical shifts contradict a relation of  $\delta^{31}\text{P}$  with atomic charges (Table 5), which indicate a partially positive phosphorus with methyl as  $\alpha$  substituent and a less charged P with methyl as “remote”,  $\beta$ -substituent (The Mulliken population analysis overemphasizes the charge difference). The obvious increase of the bond angle sum in the permethylated **1a** going along with the largest downfield shift of the NMR chemical shift relative to **1a** is in agreement with other bond angle–shift relationship studies.<sup>32</sup> Nevertheless, this relationship cannot explain the remarkable  $\beta$ -substituent effect (replacing H by CH<sub>3</sub> on endocyclic C),  $\Delta_C\delta^{31}\text{P}$ , of 79 ppm downfield. To support the argument that  $\Delta_C\delta^{31}\text{P}$  is not an effect of deformation of the local <sup>31</sup>P nucleus valence, the methyl groups in cyclo (C(CH<sub>3</sub>)<sub>2</sub>)-(PH)<sub>2</sub> were replaced by hydrogens (see footnote d in Table 5). As a result, the calculated  $\delta^{31}\text{P}$  of this deformed DPP resembles the value of **1a**. Astonishingly, the  $\alpha$  (replacing H by CH<sub>3</sub> on endocyclic P) and the  $\beta$  substituent effect seem to be additive:  $\Delta_C\delta^{31}\text{P} + \Delta_P\delta^{31}\text{P} = 85 + 79 = 164$ , which is about equal to

156 =  $\Delta_{C,P}\delta^{31}P$ . The B3LYP computed  $^{31}P$  shifts of permethylated DPP, -111 ppm, is clearly upfield relative to values derived at the same level of theory for the similarly substituted phosphorus in cyclo-1,2-(CH<sub>2</sub>)<sub>2</sub>(P-CH<sub>3</sub>)(PH) with 42 ppm (endocyclic CPP angle = 77.6) and the acyclic P(CH<sub>3</sub>)(C'H<sub>3</sub>)-(PH<sub>2</sub>) with -29 ppm (CPP angle = 98.1°, C'PP = 103.4°).

Though statistical considerations for only five values are vague, the obvious difference between the NPA, as well as Mulliken charge, at phosphorus atoms in **1a** could be established.

This lack of a charge-shift relation can also be found looking at the data for other systems.<sup>33</sup> Comparing experimental results for the three-membered ring, cyclo-(CR<sub>2</sub>)(P-Bu)<sub>2</sub> with R = H ( $\delta^{31}P$  = -168.8) and CH<sub>3</sub> ( $\delta^{31}P$  = -91.7 ppm) with the predicted chemical shifts in Table 5 shows good agreement for  $\Delta_{C}\delta^{31}P$ , the  $\beta$  substituent effect in these two similar systems.<sup>33</sup>

## Summary

The energy difference between the cyclic diphosphirene CH<sub>2</sub>-(PH)<sub>2</sub> **1** ( $E_{rel}$  = 8 kJ/mol) and the 1,2-diphospha-1-propene, **3** (global minimum) is small compared to the relative energies of 1,3-diphospha-2-propene, **2** ( $E_{rel}$  = 84 kJ/mol), 1,2-diphospha-2-propene, **4** ( $E_{rel}$  = 54 kJ/mol), and the phosphinidenes P-PH-CH<sub>3</sub> (**10**,  $E_{rel}$  = 63 kJ/mol), and P-CH<sub>2</sub>-PH<sub>2</sub> **11** ( $E_{rel}$  = 102 kJ/mol). The remarkable feature of PH-CH<sub>2</sub>-PH, a singlet minimum (**10a**) with planar tricoordinate phosphorus, is confirmed by CISD and MCSCF calculations. Although the potential intermediate products (PH-CH<sub>2</sub>-PH, PH-PH-CH<sub>2</sub>, and cyclo-CH<sub>2</sub>-PH<sub>2</sub>-P) of diphosphirane rearrangements have relative energies (182, 157, and 158 kJ/mol, respectively) slightly higher than the phosphinidene **11**, other minima of isomers were found to have  $E_{rel}$  between 287 and 322 kJ/mol. The C-H dissociation of **1a** studied by PG<sup>11</sup> turns out to be negligible compared to the homolytic cleavage of the P-H bond (more than 100 kJ/mol lower dissociation energy). Rupture of endocyclic bonds of DPP display a preference for opening the P-C bond toward the allylic CH<sub>2</sub>-PH-PH (Figure 7). The lowest energy pathway for isomerization of DPP has a barrier of 213 kJ/mol and goes via the intermediate cyclo-(CH<sub>2</sub>)(PH<sub>2</sub>)-(P) toward PH<sub>2</sub>-P=CH<sub>2</sub>. Another "shortcut" on the energy hypersurface of CH<sub>4</sub>P<sub>2</sub> is provided for the phosphorus inversion (257.9 kJ/mol, umbrella inversion mechanism) by a ring opening-ring closing mechanism with an approximately 76 kJ/mol lower barrier. Calculated energy barriers of CH<sub>3</sub>-P=PH indicate that this isomer should be kinetically stable as isolated molecule. The  $\delta^{31}P$  downfield NMR shift of 85 ppm resulting from methyl groups on carbon in place of hydrogens in **1a** is a significant  $\beta$ -substituent effect but can be rationalized by neither simple geometric nor charge arguments. Nevertheless,  $\alpha$ - and  $\beta$ -substituent effects on the NMR signal of derivatives of **1a** seem to be additive.

**Acknowledgment.** The authors thank various Flemish science foundations (FWO-Flanders, GOA-Program, and KULeuven Research Council) for continuous support.

## References and Notes

- (1) Bestmann, J.; Vostrovsky, O. *Top. Curr. Chem.* **1983**, *109*, 86-163.

- (2) Regitz, M.; S. O. J. *Multiple Bonds and Low Coordination in Phosphorus Chemistry*; Georg Thieme Verlag: Stuttgart, 1990.
- (3) Hartley, F. R. *The Chemistry of Organophosphorus Compounds*; John Wiley: New York, 1990.
- (4) Kolodiazny, O. I. *Phosphorus Ylides—Chemistry and Application in Organic Synthesis*; Wiley-VCH, Weinheim, 2000.
- (5) Etemad-Moghadam, G.; Koenig, M. *Three-Membered Rings with Two Heteroatoms including Phosphorus to Bismuth*, Vol. 1A of *Comprehensive Heterocyclic Chemistry IIA Review of the Literature 1982-1995*; Elsevier Science Ltd., Oxford, 1996.
- (6) Baudler, M.; Saykowski, F. Z. *Nat. Forsch.* **1978**, *33b*, 1208-1213.
- (7) Streubel, R.; Nieger, M.; Niecke, E. *Chem. Ber.* **1992**, *126*, 645-648.
- (8) Dransfeld, A.; Schleyer, P. v. R. *Magn. Reson. Chem.* **1998**, *36*, 29-43.
- (9) Gouygou, M.; Koenig, M.; Herve', M.-J.; Gonbeau, D.; Pfister-Guillouzo, G. *J. Org. Chem.* **1991**, *56*, 3438-3442.
- (10) Tachon, C.; Gouygou, M.; Koenig, M.; Herve', M. J.; Gonbeau, D.; Pfister-Guillouzo, G. *Inorg. Chem.* **1992**, *31*, 2414-2422.
- (11) Herve', M. J.; Etemad-Moghadam, G.; Gouygou, M.; Gonbeau, D.; Koenig, M.; Pfister-Guillouzo, G. *Inorg. Chem.* **1994**, *33*, 596-605.
- (12) Busch, T.; Schoeller, W. W.; Niecke, E.; Nieger, M.; Westermann, H. *Inorg. Chem.* **1989**, *28*, 4334-4340.
- (13) (a) Nguyen, M. T.; Landuyt, L.; Vanquickenborne, L. G. *J. Chem. Soc., Faraday Trans.* **1994**, *90*, 1770. (b) Nguyen, M. T.; Dransfeld, A.; Landuyt, L.; Vanginkenborne, L. G.; Schleyer, P. v. R., *Eur. J. Inorg. Chem.* **2000**, 103.
- (14) Dransfeld, A.; Niecke, E.; Gudat, D.; Nguyen, M. T., in preparation.
- (15) Andersson, K.; Blomberg, M. R. A.; Fülscher, M. P.; Karlström, G.; Lindh, R.; Malmqvist, P.-Å.; Neogrády, P.; Olsen, J.; Roos, B. O.; Sadlej, A. J.; Schlütz, M.; Seijo, L.; Serrano-Andrés, Siegbahn, P. E. M.; Widmark, P.-O. *MOLCAS Version 4*, Lund University, Sweden, 1997.
- (16) Wiberg, K. B. *Tetrahedron* **1968**, *24*, 1083-1096.
- (17) Frisch, M. J.; Trucks, G. W.; Schlegel, H. B.; Gill, P. M. W.; Johnson, B. G.; Robb, M. A.; Cheeseman, J. R.; Keith, T.; Petersson, G. A.; Montgomery, J. A.; Raghavachari, K.; Al-Laham, M. A.; Zakrzewski, V. G.; Ortiz, J. V.; Foresman, J. B.; Cioslowski, J.; Stefanov, B. B.; Nanayakkara, A.; Challacombe, M.; Peng, C. Y.; Ayala, P. Y.; Chen, W.; Wong, M. W.; Andres, J. L.; Replogle, E. S.; Gomperts, R.; Martin, R. L.; Fox, D. J.; Binkley, J. S.; Defrees, D. J.; Baker, J.; Stewart, J. P.; Head-Gordon, M.; Gonzalez, C.; J. A. Pople. *GAUSSIAN*. Gaussian, Inc., Pittsburgh, PA, 1995.
- (18) Wiberg, N.; Wörner, A.; Lerner, H.-W.; Karaghiosoff, K.; Fenske, D.; Baum, G.; Dransfeld, A.; Schleyer, P. *Eur. J. Inorg. Chem.* **1998**, *1*, 833-841.
- (19) Dransfeld, A. *Application of ab Initio Methods in the Investigation of Bonding and NMR Chemical Shifts of Compounds Comprising Tricoordinate Phosphorus*. Ph.D. Thesis, Erlangen, 1998.
- (20) Cowley, A. H. *Polyhedron* **1984**, *3*(4), 389-432.
- (21) Gusel'nikov, L. E.; Nametkin, N. S. *Chem. Rev.* **1979**, *79*, 529-577.
- (22) Nguyen, M. T.; Ha, T.-K. *Chem. Phys. Lett.* **1989**, *158*, 135-141.
- (23) Kapp, J.; Schade, C.; El-Nahasa, A. M.; Schleyer, P. v. R. *Angew. Chem., Int. Ed. Engl.* **1996**, *35*, 2236-2238.
- (24) Nguyen, M. T.; Van Keer, A.; Ha, T.-K.; Vanquickenborne, L. G. *Theochem (J. Mol. Struct.)* **1994**, *130*, 125-134.
- (25) Minkin, V. I.; Glukhovtsev, M. N.; Simkin, B. Y.; *Aromaticity and Antiaromaticity—Electronic and Structural Aspects*; John Wiley: New York, 1994.
- (26) Benson, S. W. *Thermochemical Kinetics*; John Wiley: New York, 1976.
- (27) Schleyer, P. v. R.; Kost, D. *J. Am. Chem. Soc.* **1988**, *110*, 2105-2109.
- (28) Boyd, S. L.; Boyd, R. J.; Bessonette, P. W.; Kerdraon, D. I.; Aucoin, N. T. *J. Am. Chem. Soc.* **1995**, *117*, 8816-8822.
- (29) Boyd, S. L.; Boyd, R. J. *J. Am. Chem. Soc.* **1997**, *119*, 4214-4219.
- (30) Schoeller, W. W. Bonding Properties of Low Coordinated Phosphorus Compounds. In *Multiple Bonds and Low Coordination in Phosphorus Chemistry*; Georg Thieme Verlag: Stuttgart, 1990.
- (31) Kutzelnigg, W. *Angew. Chem., Int. Ed. Engl.* **1984**, *23*, 272.
- (32) Hahn, J.; Baudler, M.; Krüger, C.; Tsay, Y.-H. Z. *Naturforsch.* **1982**, *37b*, 797-805.
- (33) Bühl, M.; Schleyer, P. v. R. *Inorg. Chem.* **1991**, *30*, 3107-3111.
- (34) Reed, A. E.; Curtis, L. A.; Weinhold, F. *Chem. Rev.* **1988**, *88*, 899-926.